

Electronic Supplementary Information

Efficiently direct methane to methanol on CuZn hetero- diatomic catalysts with certain coordination spheres: A DFT study

Chunhua Yang,^a Cailong Liu,^b Yuxiu Wang,^c He-Na Zhang,^a Qi-Wen He,^a Dai-Song
Tang^a and Xiao-Chun Wang^{*a}

^a *Institute of Atomic and Molecular Physics, Jilin University, Changchun, 130012,
P.R. China.*

^b *School of Physics Science and Information Technology, Liaocheng University,
Liaocheng, 252000, P.R. China.*

^c *School of Ecology and Environment, Yuzhang Normal University, Nanchang,
330103, P.R. China.*

*Corresponding Author: wangxiaochun@jlu.edu.cn

Formation energy (E_f), binding energy (E_b) and dissolution potential (U_{diss})

In order to adopt the optimal coordination configurations of the CuZn atoms embedded in nitrogen-decorative graphene, the formation energy (E_f) of CuZn-NG is calculated by using the Eq. S1 [S1,S2]:

$$E_f = E_{CuZn-NG} + 10 \mu_C - (E_{Gra} + 6\mu_N + \mu_{Cu} + \mu_{Zn}) \quad (\text{Eq. S1})$$

where $E_{CuZn-NG}$ is the total energy of CuZn-NG, E_{Gra} is the total energy of the pristine 6×6 graphene supercell and μ_C is the chemical potential of C atom [S3,S4], and μ_N is the chemical potential of N atom taken from a N_2 molecule in the gas phase [S5]. μ_{Cu} and μ_{Zn} are the chemical potentials of Cu and Zn atoms, respectively [S6].

In order to verify that the combination of CuZn atoms is favorable, the binding energy () between the two Cu atoms or two Zn atoms or CuZn atoms and the substrate is studied and defined as Eq. S2 [S7]:

$$E_b = E_{CuZn-NG} - E_{Cu} - E_{Zn} \quad (\text{Eq. S2})$$

where and represent the total energies of CuZn-NG and NG, respectively,

/ is the total energy of a Cu/Zn atom in the most stable bulk structure.

In addition, to evaluate the stability of the system in electrode working conditions, the dissolution potential () is calculated as Eq. S3 [S8]:

$$U_{diss} = U_{diss}^0(\text{metal, bulk}) - E_b/N_e \quad (\text{Eq. S3})$$

where (metal, bulk) is the standard dissolution potential of the bulk metal, is the number of transferred electrons during the dissolution.

Table S1 Binding energy (), standard dissolution potentials () of metals, number of transferred electrons () during the dissolution and dissolution potential () of metals.

Species	(eV)	(V)		(V)
CuCu-N _P G	-1.99	0.34	2	0.84
ZnZn-N _P G	-3.15	-0.76	2	0.03
CuZn-N _P G	-2.94	0.34/-0.76	2/2	0.37/0.08
CuCu-N _{PA} G	-4.17	0.34	2	1.38
ZnZn-N _{PA} G	-5.22	-0.76	2	0.55
CuZn-N _{PA} G	-5.01	0.34/-0.76	2/2	1.16/0.42

Table S2 The atomic charge ($|e|$) of first CS and second CS in NG and CuZn-NG. The atomic charge changes ($\Delta|e|$) of first CS and second CS when CoNi atoms embedded in NG.

		N _P G	CuZn-N _P G	N _{PA} G	CuZn-N _{PA} G
$ e $	first CS	-6.90	-7.61	-5.60	-7.26
	second CS	7.12	5.79	5.73	5.31
$\Delta e $	first CS		-0.71		-1.66
	second CS		-1.33		-0.42

Table S3 Adsorption energy (E_{ads}) of H₂O and H₂O₂ molecule.

Species		E_{ads} (eV)
CuZn-N _P G	H ₂ O ₂	-0.33
	H ₂ O	-0.41
CuZn-N _{PA} G	H ₂ O ₂	-0.28
	H ₂ O	-0.33

Table S4 The atomic charge ($|e|$) and d-band center (eV) during methane oxidation to methanol.

Species	d-band center of Cu (eV)	d-band center of Zn (eV)	Atomic charge of Cu ($ e $)	Atomic charge of Zn ($ e $)
CuZn-N _p G (I)	-2.93	-7.27	0.60	1.02
II	-2.96	-7.06	0.64	1.08
III	-2.59	-5.70	0.90	1.19
IV	-2.48	-5.70	0.88	1.18
V	-2.50	-5.70	0.88	1.18
VI	-2.15	-6.23	0.77	1.16
VII	-2.74	-6.95	0.61	1.09
CuZn-N _{PA} G (I)	-4.27	-6.52	0.94	1.18
II	-4.30	-6.40	0.95	1.22
III	-3.82	-5.43	0.99	1.24
IV	-3.73	-5.52	1.01	1.22
V	-3.78	-5.48	1.00	1.22
VI	-3.94	-4.95	0.95	1.24
VII	-4.29	-6.15	0.95	1.24

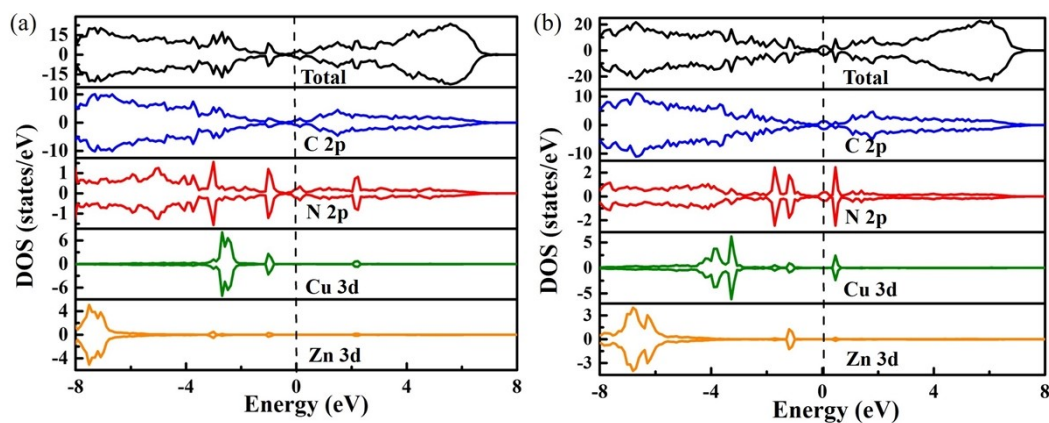


Fig. S1 Spin-polarized density of states for (a) CuZn-N_pG, (b) CuZn-N_{PA}G.

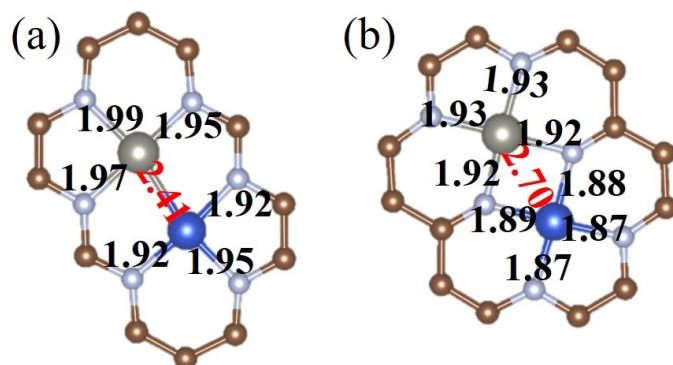


Fig. S2 The geometric structures and the mainly bonds lengths (Å) of (a) CuZn-N_pG and (b) CuZn-N_{pA}G.

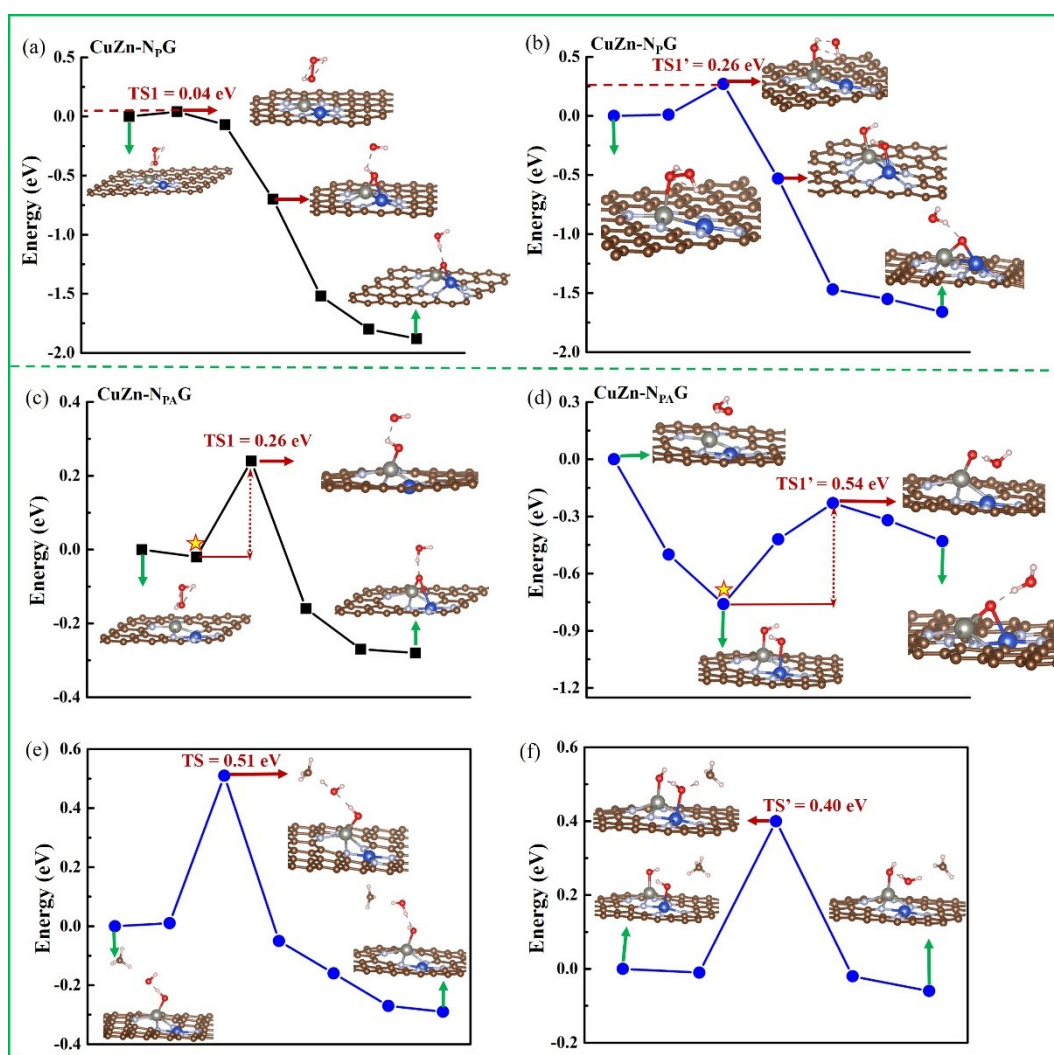


Fig. S3 Reaction pathway for H₂O₂ oxidizes CuZn atoms on (a, b) CuZn-N_pG, and (c, d) CuZn-N_{pA}G. The reaction pathway of (e, f) OH* activation of CH₄.

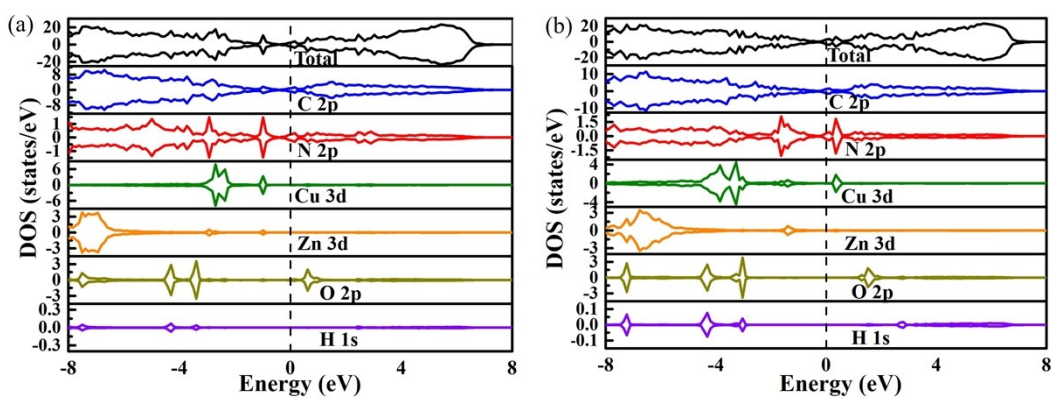


Fig. S4 Spin-polarized density of states for (a) CuZn-N_pG, (b) CuZn-N_{pA}G after adsorption H₂O₂ (II-state).

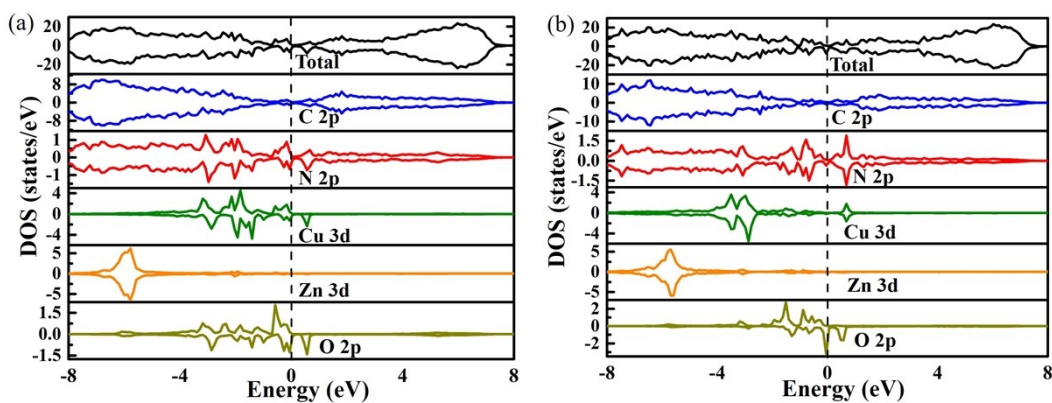


Fig. S5 Spin-polarized density of states for (a) CuZn-N_pG-O, (b) CuZn-N_{pA}G-O (IV-state).

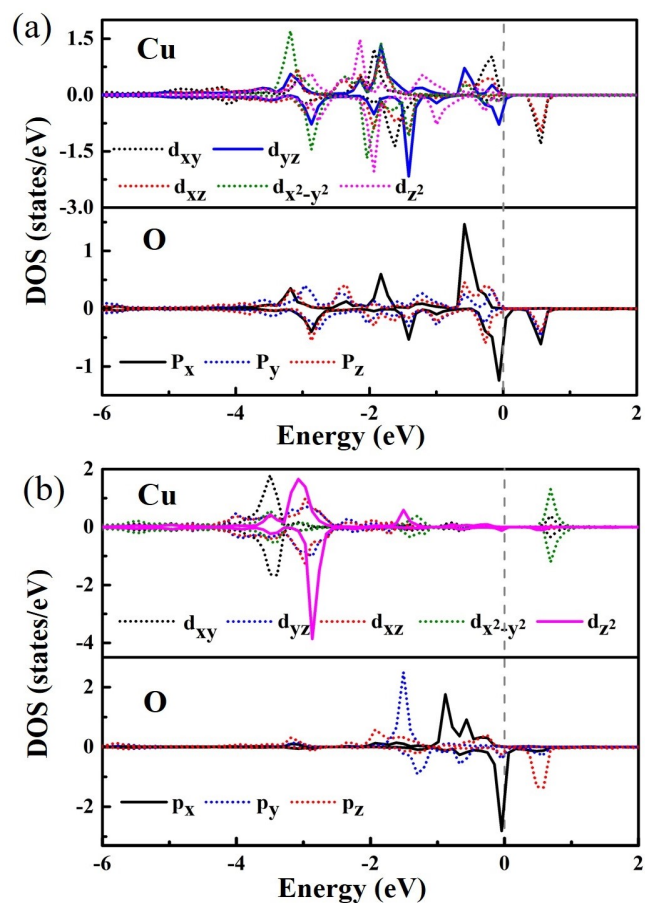


Fig. S6 Spin-polarized density of states of Cu 3d and O 2p split orbitals for (a) CuZn-N_pG-O, (b) CuZn-N_{pA}G-O (IV-state).

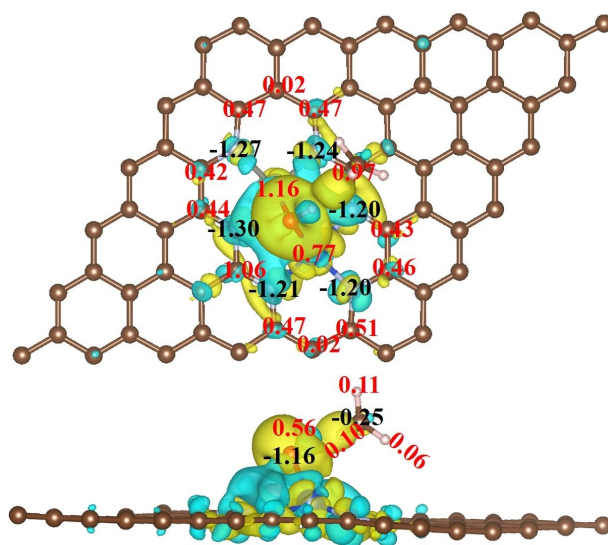


Fig. S7 The Bader charge analysis and the 3D charge density differences for CuZn-N_pG after the activation of C-H bond (VI-state), the isosurface value is 0.003 e bohr⁻³.

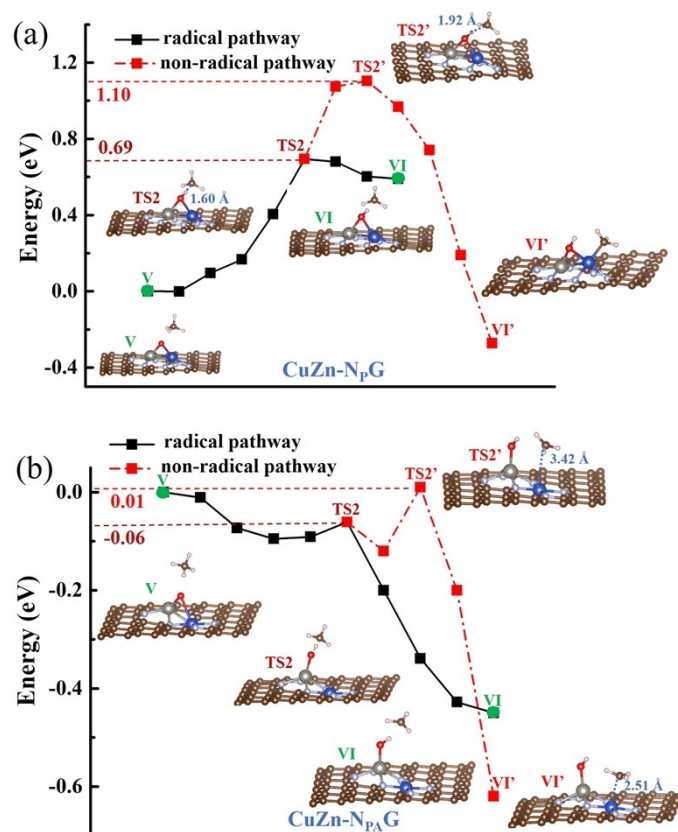


Fig. S8 The radical pathway and non-radical pathway for methane oxidation on (a) CuZn-N_pG-O and (b) CuZn-N_{pA}G-O.

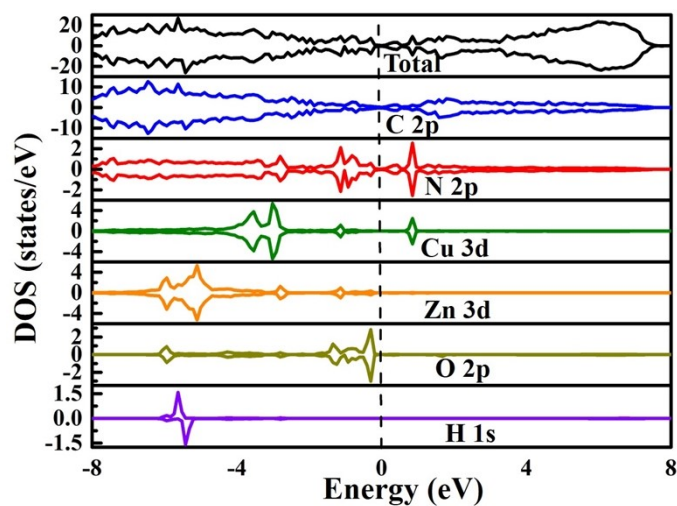


Fig. S9 Spin-polarized density of states for CuZn-N_{pA}G after the activation of C-H bond (VI-state).

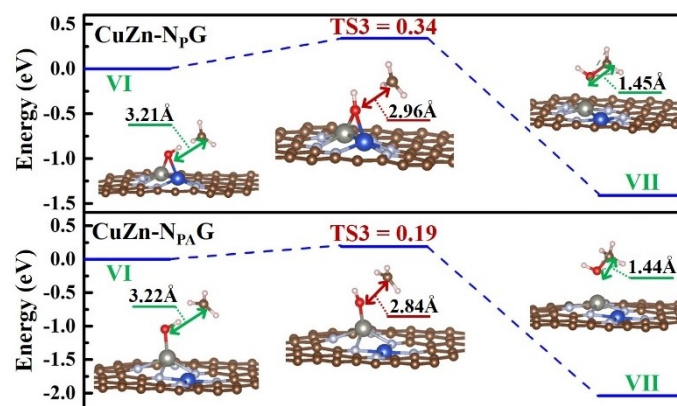


Fig. S10 Energy profile of methanol formation reaction as well as the structures of TS3, VI- and VII-state.

Table S5 ΔE (eV), energy difference between X-state and I-state, X= II, TS1, V, TS2,VI, TS3. Atomic charge of Cu center ($|e|$), energy barrier (eV) and change in atomic charge of Cu center ($|e|$).

Species	ΔE (eV)	Atomic charge of Cu ($ e $)	Energy barrier (eV)	Change in atomic charge of Cu ($ e $)
CuZn-N_pG(II)	-0.33	0.64		
TS1	-0.29	0.63	0.04	-0.01
V	-1.99	0.88		
TS2	-1.30	0.79	0.69	-0.09
VI	-1.40	0.77		
TS3	-1.06	0.74	0.34	-0.03
CuZn-N_{pA}G(II)	-0.28	0.95		
TS1	-0.04	0.97	0.26	0.02
V	-0.30	1.00		
TS2	-0.36	0.96	-0.06	-0.04
VI	-0.74	0.95		
TS3	-0.55	0.96	0.19	0.01

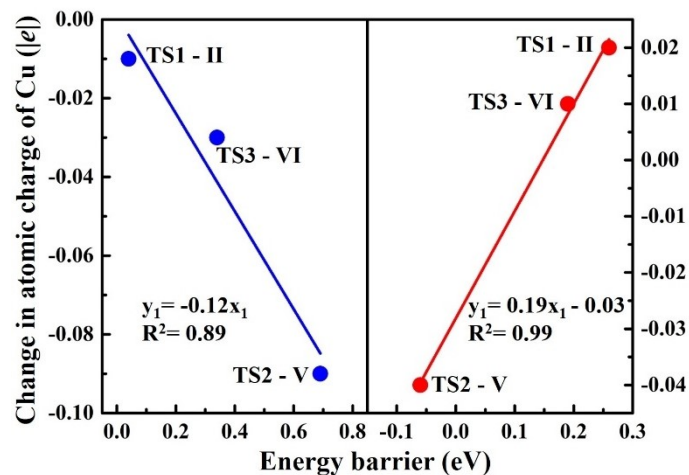


Fig. S11 The relationship between change in atomic charge of Cu center and energy barrier.

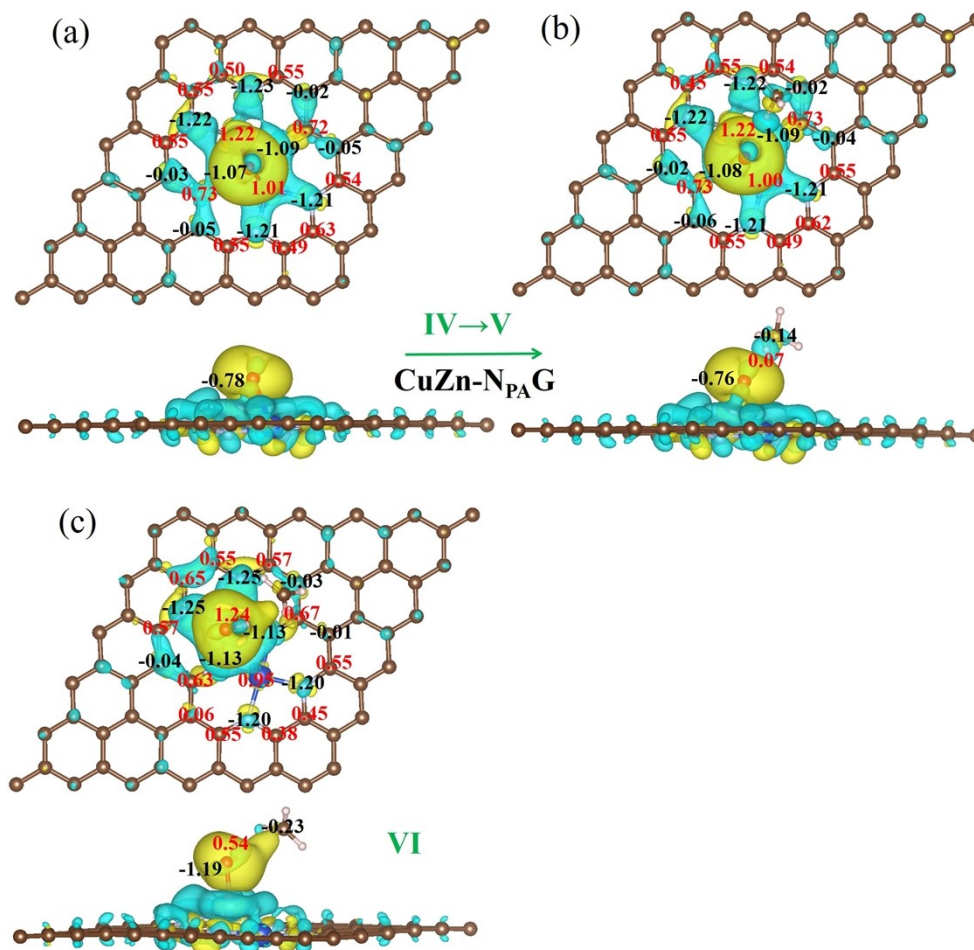


Fig. S12 Bader charge analysis and the 3D charge density differences of CuZn-N_{PA}G at (a) IV, (b) V and (c) VI-state, the isosurface value is 0.003 e bohr⁻³.

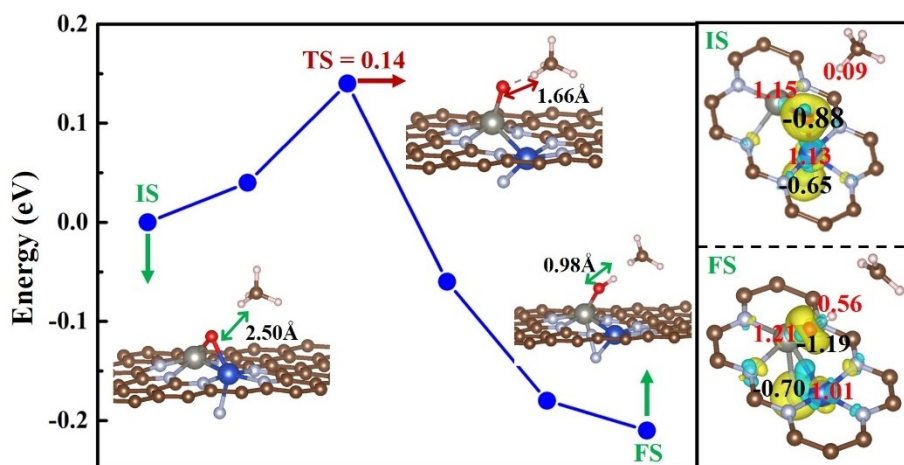


Fig. S13 Reaction pathway for methane activation on F-CuZn-N_pG-O. The Bader charge analysis and the 3D charge density differences for initial structure (IS) and final structure (FS), the isosurface value is 0.005 e bohr⁻³.

References

- [S1] L. Liu, C. Chen, L. Zhao, Y. Wang, X. Wang, *Carbon*, 2017, **115**, 773-780.
- [S2] Y. Wei, L. Sun, M. Wang, J. Hong, L. Zou, H. Liu, et al. *Angew Chem. Int. Edit.*, 2020, **59**, 16013-16022.
- [S3] L. Ismer, M. Park, A. Janotti, C. Van de Walle, *Phys. Rev. B*, 2009, **80**, 184110.
- [S4] C. Van de Walle, J. Neugebauer, *J. Appl. Phys.*, 2004, **95**, 3851-3879.
- [S5] E. Finazzi, C. Di Valentin, A. Selloni, G. Pacchioni, *J. Phys. Chem. C*, 2007, **111**, 9275-9282.
- [S6] S. Kattel, P. Atanassov, B. Kiefer, *Phys. Chem. Chem. Phys.*, 2014, **16**, 13800-13806.
- [S7] C. Zhang, S. Qin, B. Li, P. Jin, *J. Mater. Chem. A*, 2022, **10**, 8309-8323.
- [S8] X. Guo, J. Gu, S. Lin, S. Zhang, Z. Chen, S. Huang, *J. Am. Chem. Soc.*, 2020, **142**, 5709-5721.